

Supplemental Information

Age-Associated Loss of OPA1 in Muscle

Impacts Muscle Mass, Metabolic Homeostasis,

Systemic Inflammation, and Epithelial Senescence

Caterina Tezze, Vanina Romanello, Maria Andrea Desbats, Gian Paolo Fadini, Mattia Albiero, Giulia Favaro, Stefano Ciciliot, Maria Eugenia Soriano, Valeria Morbidoni, Cristina Cerqua, Stefan Loeffler, Helmut Kern, Claudio Franceschi, Stefano Salvioli, Maria Conte, Bert Blaauw, Sandra Zampieri, Leonardo Salviati, Luca Scorrano, and Marco Sandri

Fig. S1

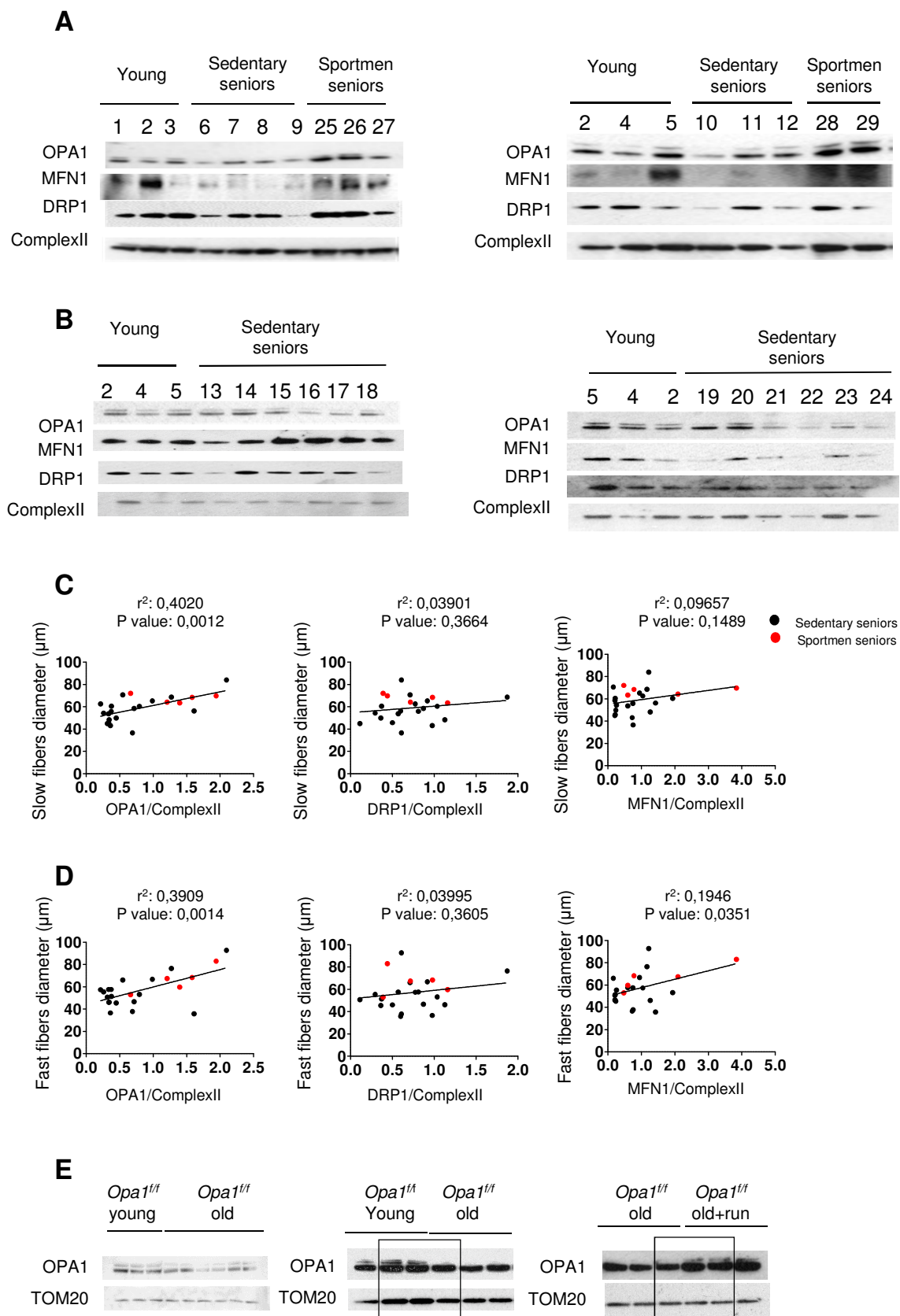


Figure S1 – OPA1 expression is reduced during ageing in sarcopenic patients - Related to Figure 1

A-B) Immunoblots of human muscle homogenates. On the top of each blot is indicated the number of the relative sample loaded. Further information related to the subjects can be find in the supplementary tables S1 and S2. MNF1, OPA1 and DRP1 were normalized for complex II expression levels. **C-D)** Linear regression analysis between OPA1, DRP1 and MFN1 expression levels and slow (C) and fast (D) myofiber size in elderly persons, (n=23) **E)** Uncropped scans of the western blots presented in Figure 1E. Muscle homogenates of tibialis anterior muscles from young, old and old trained mice were immunoblotted for the indicated antibodies. young (6 months-old n=6), old (18 months-old n=9) and old trained mice (18 months-old n=6).

Fig. S2

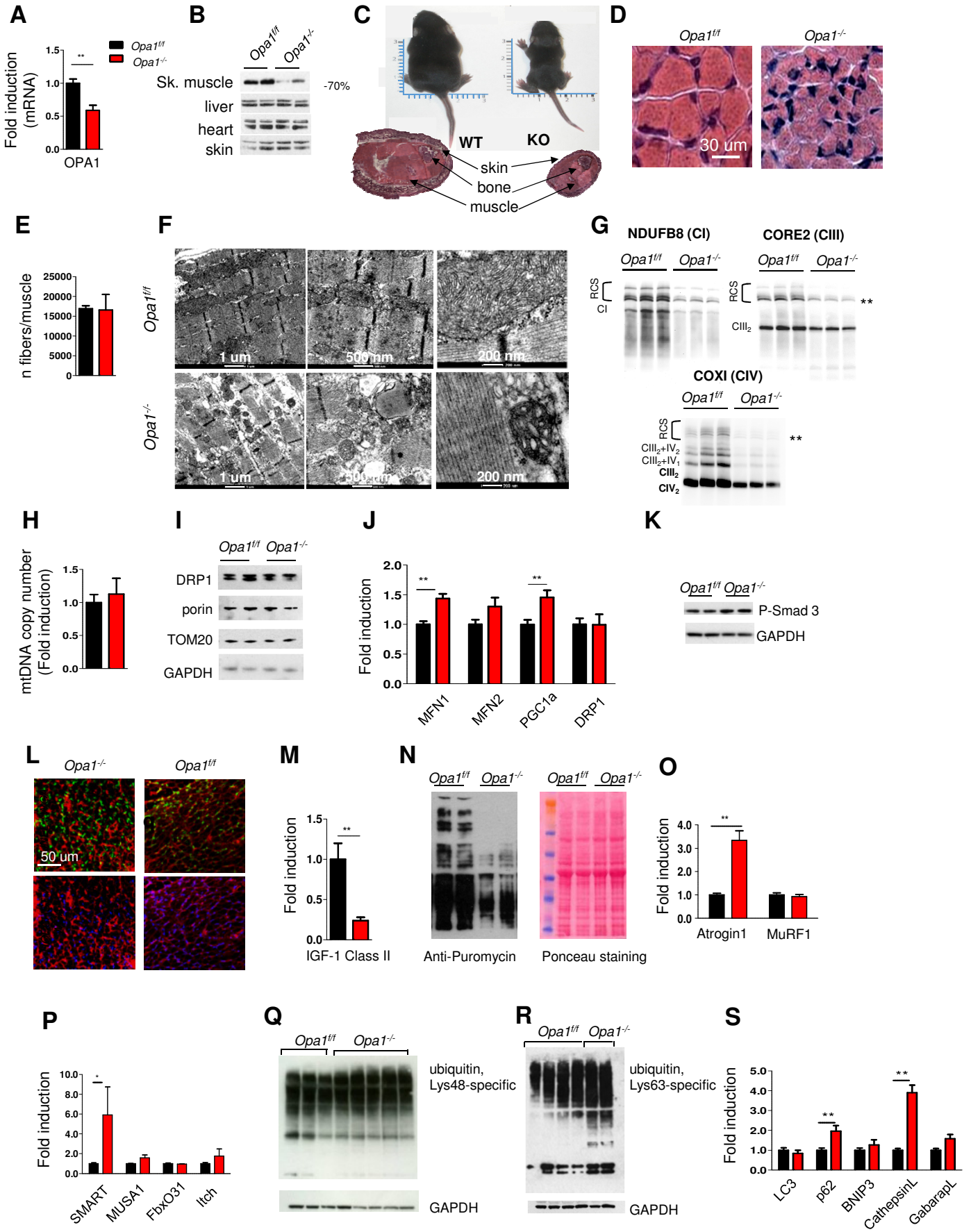


Figure S2- OPA1 deletion affects mitochondria morphology and function, muscle stem cell renewal, protein synthesis and protein breakdown inducing defects in muscle growth and a lethal phenotype - Related to Figure 2

A) OPA1 mRNA and **B)** OPA1 protein levels are downregulated in skeletal muscle and not in other tissues in OPA1-null mice. Each condition represents the mean \pm SEM of at least three independent experiments **C)** Upper row: Representative photograph of control and KO littermates at post-natal day 8 showing that *OPA1*^{-/-} mice are smaller than controls. Lower row: Haematoxylin-Eosin (HE) staining of hindlimb cross-section **D)** HE staining of muscles reveals smaller fibers in OPA1 knockout than controls (n=5 per each) **E)** Total number of fibers per muscle. Data represent mean \pm SEM (n=4) **F)** Representative electron micrographs of gastrocnemius muscles from MLCOPA1^{+/f} (upper row) and MLCOPA1^{-/-} (lower row). OPA1 deletion leads to altered sarcomeric organization (left panel), lipid droplets accumulation (middle panel) and defects in cristae shape (right panel). Scale bar is indicated at the bottom of each picture **G)** OPA1 deficiency leads to a significant reduction of CIII and CIV assembly in respiratory chain supercomplexes (RCS). Representative Blue Native-PAGE analysis showing RCS developed and normalized for individual respiratory chain complexes. CI subunit NDUFB8 (left panel), CIII-Core2 protein 2 (right panel) and CIV subunit COXI (bottom panel) **H)** Mitochondrial DNA copy number is not affected by OPA1 deletion. Data are normalized to controls; data are mean \pm SEM, n=5 **I)** Representative immunoblots for mitochondrial proteins of three independent experiments of muscle homogenates **J)** qRT-PCR revealed changes in expression of different pro-fusion and fission genes. Data are mean \pm SEM (n=6) **K)** Phosphorylation of Smad3, revealed no changes in myostatin pathway between controls and OPA1 knockout. Data are mean \pm SEM (n=5) **L)** Representative images of TUNEL assay. Similar number of TUNEL positive nuclei per muscles in control and OPA1 knock-out animals was observed (n=5 per each) **M)** qRT-PCR revealed a decrease of IGF-1 expression in the liver of OPA1 knockout mice (n=5) **N)** *In vivo* SUnSET technique demonstrate a significant reduction of protein synthesis in OPA1-ablated mice muscles. Data are mean \pm SEM of three independent experiments **O)** qRT-PCR analysis of transcriptional levels of the FoxO-target genes: Atrogin1 and MuRF1 and **P)** SMART, MUSA1, FbxO31 and Itch **Q)** Representative western blots of Lysine 48 (Lys48) and **R)** Lysine 63 (Lys63) poly-ubiquitinated proteins of muscle extracts from controls and OPA1 knockout mice **S)** Transcriptional levels of several autophagy-related genes. Data are mean \pm SEM (n=6 per condition) Statistical significance: *p \leq 0,05; **p \leq 0,01 and ***p \leq 0,001. CI: Complex I; CIII: Complex III; CIV: Complex IV; CIII₂+CIV₂: Complex III₂ plus Complex IV₂; CIII₂+CIV₁: Complex III₂ plus Complex IV₁.

Fig. S3

MLC OPA1- CONDITIONAL MODEL

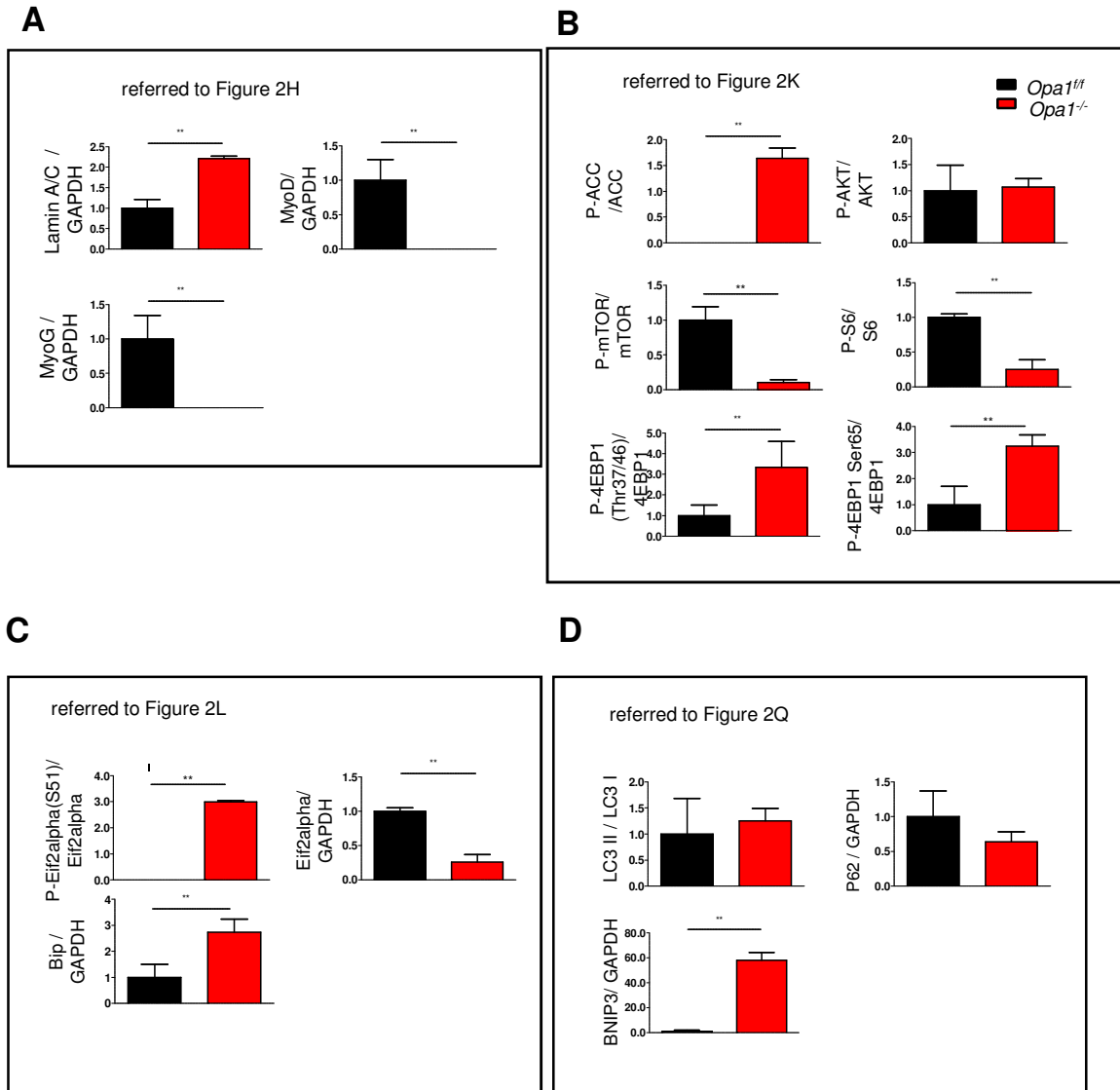


Figure S3 - Densitometric quantification of the western blots related to Figure 2

Fig. S4

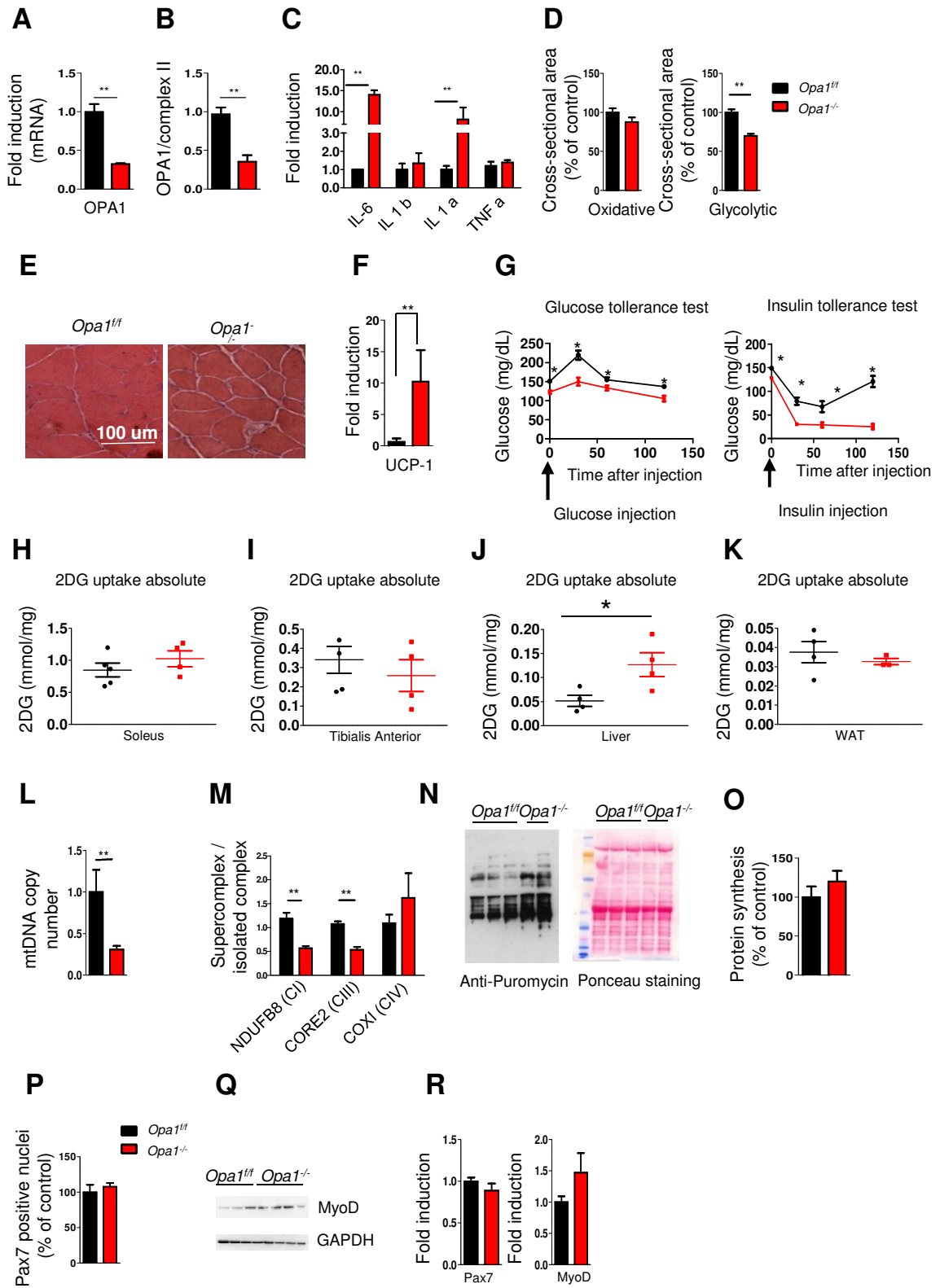


Figure S4- Acute deletion of OPA1 in adult muscles reverberates to whole body leading to metabolic changes and to mitochondrial dysfunction - Related to Figure 3 and to Figure 4

A) OPA1 mRNA and **B)** OPA1 protein levels are downregulated in skeletal muscle after tamoxifen-dependent OPA1 deletion. Each condition represents the mean of at least three independent experiments \pm SEM **C)** Blood levels of the inflammatory cytokines IL6, IL1a, IL1b and TNFa **D)** Cross-sectional area quantification of both, oxidative and glycolytic fibers in controls and in OPA1-null mice **E)** Representative HE staining of *Opa1^{fl/fl}* and *Opa1^{-/-}* mice showing normal morphology, absence of inflammation and no signs of degeneration **F)** qRT-PCR of UCP-1 expression in WAT of *Opa1^{fl/fl}* and *Opa1^{-/-}* **G)** Glucose and Insulin tolerance tests performed in *Opa1^{fl/fl}* and *Opa1^{-/-}* mice are shown. Data are mean \pm SEM of three independent experiments **H-I-J-K)** Graphs show 2-deoxyglucose uptake in vivo in Soleus, Tibialis Anterior, Liver and WAT **L)** Mitochondrial DNA copy number is affected by OPA1 deletion. Data are normalized to controls; (n=3) **M)** OPA1 deficiency leads to a significant reduction of CIII and CIV assembly in respiratory chain supercomplexes (RCS). Quantification of Blue Native-PAGE analysis showing RCS developed and normalized for individual respiratory chain complexes : CI subunit NDUFB8 CIII-Core2 protein 2 and CIV subunit COXI **N)** *In vivo* SUnSET measurements showing no differences of protein synthesis between control and OPA1-deficient adult muscles **O)** Quantification of puromycin-labeled peptides, expressed as a percentage of the values obtained in the control group. Data are mean \pm SEM of three independent experiments **P)** Pax7 positive muscle stem revealed by immunohistochemistry and normalized for muscle area and **Q)** MyoD levels detected by western blot (n=4) **R)** qRT-PCR for Pax7 and MyoD expression in adult skeletal muscles of *Opa1^{fl/fl}* and *Opa1^{-/-}*; (n=3) Statistical significance; *p \leq 0,05 and **p \leq 0,01. CI: Complex I; CIII: Complex III; CIV: Complex IV.

Fig. S5

HSA OPA1- INDUCIBLE MODEL

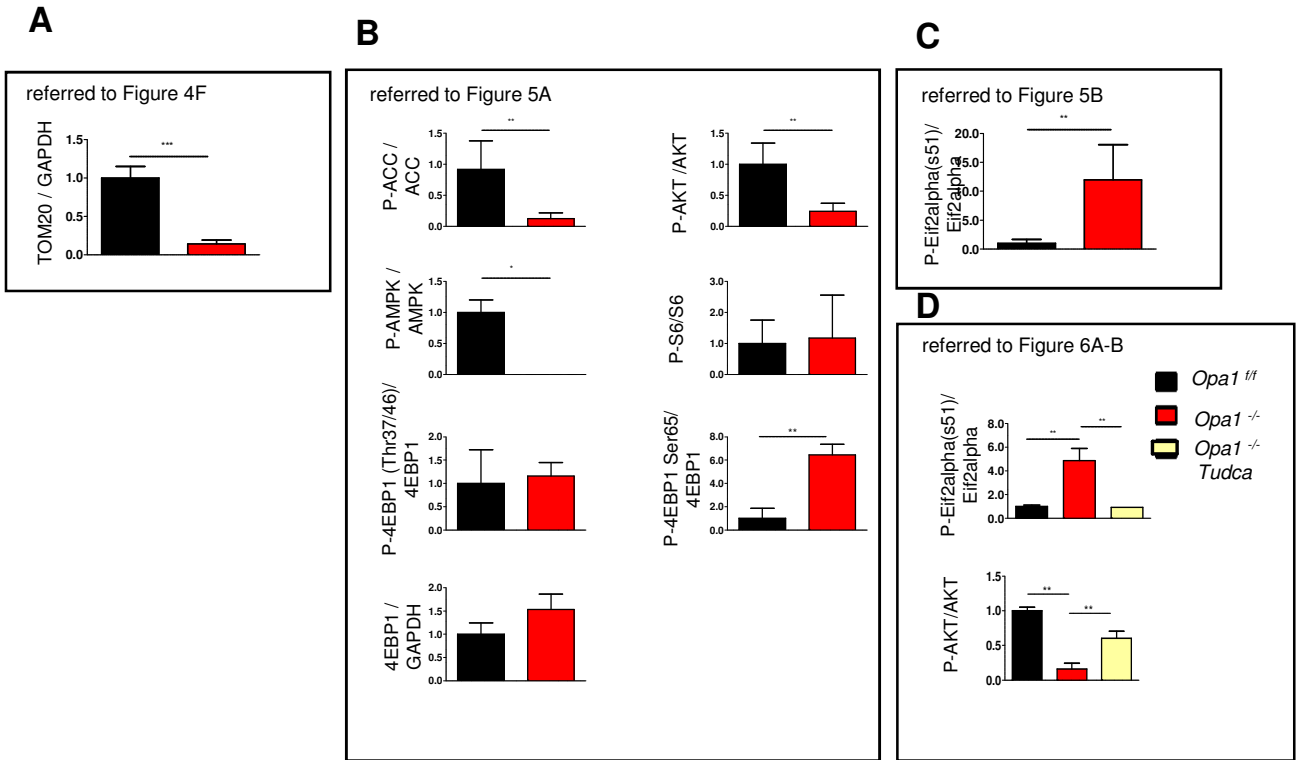


Figure S5 - Densitometric quantification of the western blots related to Figure 4, Figure 5 and Figure 6

Fig. S6

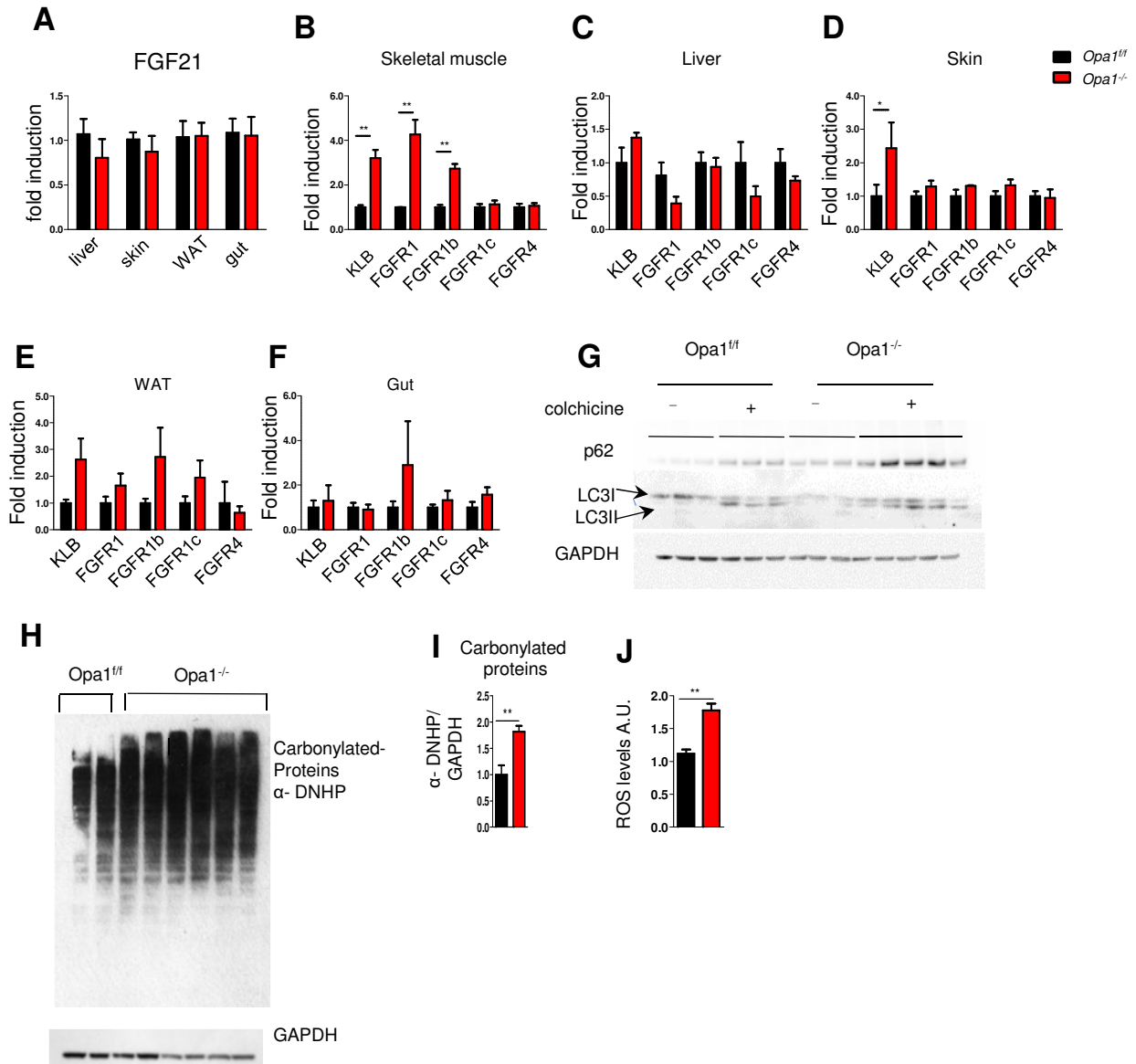


Figure S6 - FGF21, Klotho, FGF Receptors, oxidative stress and autophagy flux in OPA1 knockout mice - Related to Figure 5

A) qRT-PCR revealed no changes in FGF21 expression levels in the different tissues analyzed **B-F)** qRT-PCR for different FGF receptors isoforms and KBL in skeletal muscle, liver, skin, WAT and gut (n=6 per each condition per tissue) **G)** Autophagy flux is increased in basal condition in OPA1-deficient muscles. Inhibition of autophagosome–lysosome fusion by colchicine treatment induces more accumulation of p62 and LC3II band in OPA1-null muscles (n=10 per each condition) **H)** Representative oxyblot of *Opal^{fl/fl}* and *Opal^{-/-}* samples and **I)** its relative quantification **J)** Mitochondrial oxidative stress analysis, measured with Mt-roGFP1 sensor. Statistical significance: *p≤ 0,05 and **p≤ 0,01 (n =20 fibers per each condition)

Fig. S7

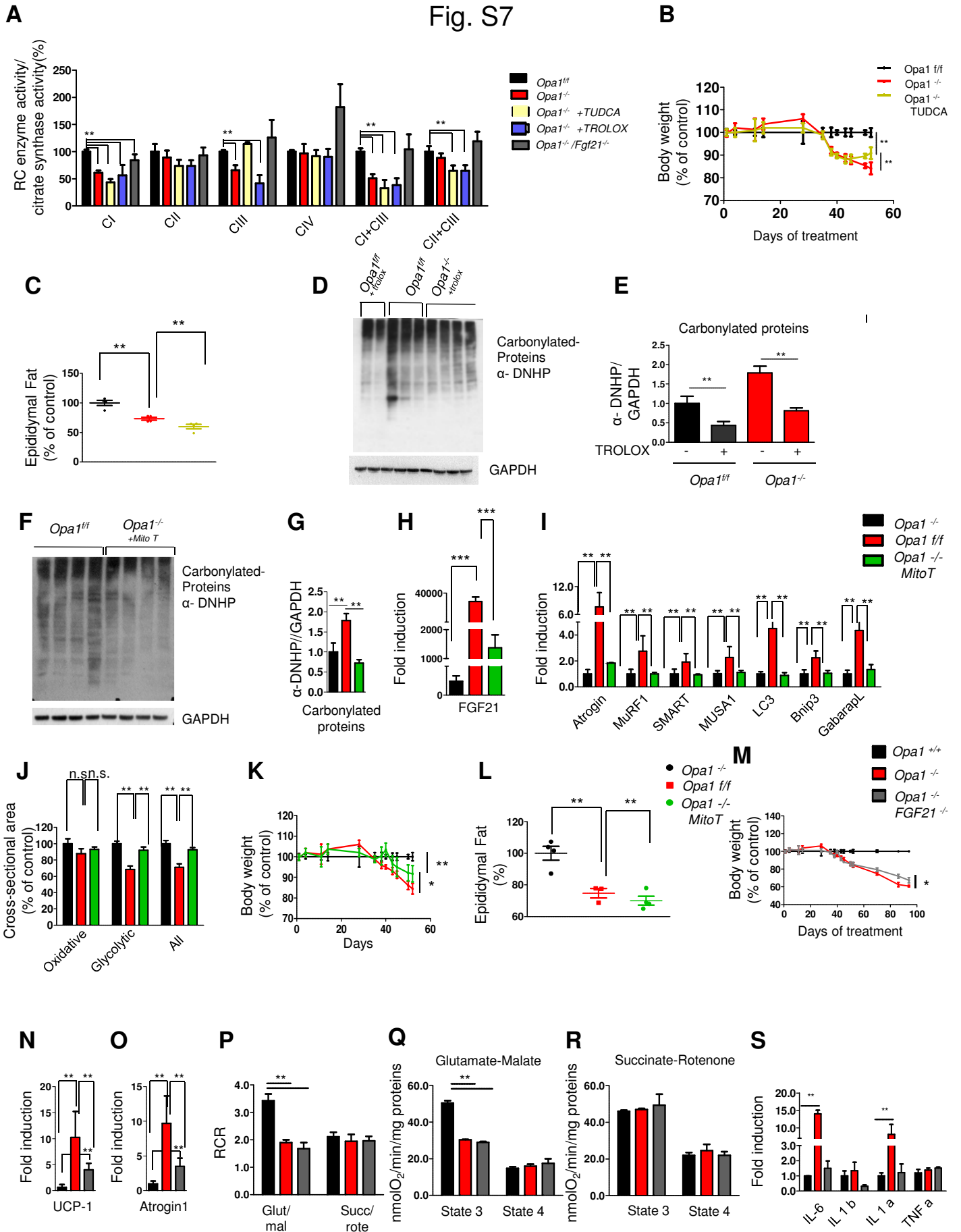


Figure S7 - Trolox, MitoTempo, TUDCA treatments and acute deletion of FGF21 ameliorate the phenotype of OPA1^{-/-} mice - Related to Figure 6 and to Figure 7

A) Respiratory Complex (RC) enzyme activity normalized for citrate synthase for *Opal^{ff}*, *Opal^{-/-}*, *Opal^{-/-}+TUDCA*, *Opal^{-/-}+TROLOX*, *Opal^{-/-}/Fgf21^{-/-}* **B)** Growth curve of control and *Opal^{-/-}* mice treated or not with the chemical chaperone TUDCA after tamoxifen treatment; (*Opal^{ff}* n=20, *Opal^{-/-}+ vehicle* n=19, *Opal^{-/-}+ TUDCA* n= 8) **C)** Epididymal fat content measurement (n=4) **D)** Representative oxyblot for TROLOX treatment and **E)** its quantification. Data are mean ± SEM of n= 6 for each condition **F)** Oxyblot of *Opal^{ff}* and *Opal^{-/-}+ mito-TEMPO* and **G)** its relative quantification **H)** Fgf21 transcriptional levels are reduced in OPA-null mice treated with mito-TEMPO **I)** qRT-PCR of FoxO- target genes. Data are mean ± SEM of three independent experiments **J)** Quantification of cross-sectional area of myofibers from controls, OPA1-knockout and OPA1-deficient mice treated with mito-TEMPO. Values are mean ± SEM from at least 6 muscles in each group **K)** Growth curve after tamoxifen treatment of control, OPA1^{-/-} and OPA1-null mice treated with mito-TEMPO. Data are mean ± SEM (*Opal^{ff}* n=20, *Opal^{-/-}*n=19 and *Opal^{-/-}+ mito-TEMPO* n=9) **L)** WAT loss is not prevented by mito-TEMPO treatment **M)** Partial protection from body weight loss in *Opal^{-/-}/Fgf21^{-/-}* double knockout mice; (*Opal^{ff}* n=20, *Opal^{-/-}*n=19 and *Opal^{-/-}/Fgf21^{-/-}* n=10) **N)** qRT-PCR of UCP-1 expression in WAT of *Opal^{ff}*, *Opal^{-/-}* and *Opal^{-/-}/Fgf21^{-/-}* is shown. Data are mean ± SEM of three independent experiments **O)** Atrogin1 transcriptional levels in skeletal muscles of *Opal^{ff}*, *Opal^{-/-}* and *Opal^{-/-}/Fgf21^{-/-}* is shown. Data are mean ± SEM of three independent experiments **P)** Respiratory control ratio of muscle isolated mitochondria energized with 5mM/2,5mM GLU/MAL or 10mM SUCC. Data represent mean ± SEM of three independent experiments (n=5) **Q-R)** State III and IV of muscle isolated mitochondria energized 5mM/2,5mM GLU/MAL or 10mM SUCC Data represent mean ± SEM of three independent experiments (n=5). **S)** Transcriptional levels of the inflammatory cytokines IL6, IL1a, IL1b and TNFα in skeletal muscle. Statistical significance: *p≤ 0,05 and **p≤ 0,01 n.s.: not significant CI: Complex I; CII: Complex II; CIII: Complex III; CIV: Complex IV; CI+CIII: Complex I plus Complex III; CII+CIII: Complex II plus Complex III

Supplemental tables

Table. S1. Related to Human subjects Fig 1 and S1

		Biopsy number	Age (y)	Weight (kg)	Height (cm)	BMI	TUGT (s)	Maximal isometric torque (Nm/kg)	Weekly training (h)	VAS	WOMAC	
SENIORS	YOUNG	1	27,76944	77	176	24,85795	3,7	4,10	7	0	1,00	
		2	23,24167	81	177	25,85464	4,1	2,95	7,5	0	1,00	
		3	34,21667	66	172	22,30986	3,95	3,36	5	0	1,00	
		4	25,13333	75	169	26,25958	4	2,93	6	0	1,00	
		5	26,25278	70,1	179	21,87822	4,1	2,69	3,375	0	1,00	
	Sedentary	6	67,63288	80	172	27,04164	7,8	1,74	0	0	n/a	
		7	69,45205	72	171	24,62296	6,9	1,67	0	2,1	n/a	
		8	70,32877	96	190,5	26,45339	8,53	2,24	0	0	1,07	
		9	70,60548	95	185	27,75749	5,3	2,01	0	4	3,46	
		10	77,70685	118,3	182	35,71429	9,46	1,46	0	0,5	1,96	
		11	66,92877	93,5	181	28,54003	4,68	1,70	0	0	2,29	
		12	81,89041	89,6	186	25,89895	9,32	1,13	0	0,85	n/a	
		13	67,12295	85	181	25,94548	5,9	2,14	0	2,7	3,04	
		14	63,39617	83,6	174	27,61263	7,3	1,14	0	5,7	2,88	
		15	68,94536	71	182	21,43461	6	1,69	0	3,7	2,96	
		16	64,59563	85	187	24,30724	5,9	1,34	0	7,9	3,58	
		17	74,88525	68	160	26,5625	6,7	1,03	0	8,2	5,25	
		18	79,39071	72,2	162	27,51105	12	0,87	0	8,4	4,50	
		19	53,21311	75	150	33,33333	15,4	1,01	0	8,4	7,08	
		20	65,46175	72	168	25,5102	9	0,90	0	7,1	4,83	
		21	67,87705	98	176	31,6374	14,3	0,68	0	8,5	6,17	
		22	62	116	171	39,7	6,7	0,66	0	8,5	6,16	
		23	75,9153	88	170	30,44983	9,1	0,85	0	8,3	5,63	
		24	78,7623	65	150	28,88889	12,2	0,78	0	7,2	3,88	
		Sportmen	25	69,2	73,6	176,0	23,8	4	2,49	16	2,1	2,46
			26	72,3	92,0	180,0	28,4	5	2,18	10	0	1,00
			27	67,0	76,0	174,0	25,1	4,1	2,33	7	0,9	1,21
			28	69,5	81,6	169,5	28,4	5,4	1,98	4,5	0	1,00
			29	66,0	99,0	184,0	29,2	4,34	2,17	9	0	1,00

Table. S2. Related to Human subjects Fig 1 and S1

Criteria	YOUNG	SENIORS	
	n=5	Sedentary n=19	Sportsmen n=5
AGE (y)	27,32 ± 4,19	69,8±7,04 *	68,80±2,42 *
WEIGHT (kg)	73,82 ± 5,87	85,4±15,04	84,4±10,79
HEIGHT (cm)	174,6 ±4,04	173,6±11,78	176,70±5,56
BMI (kg/m ²)	24,23±2,02	28,2±4,29	27±2,39
TUGT (s)	4±0,16	8,65±3,02 *	4,6±0,60 #
Maximal isometric torque Nm/kg	3,21±0,56	1,30±0,50 *	2,20±0,19 *, #
Weekly training (h)	5,80±1,65	0 *	9,3±4,29 #
VAS	0	4,85±3,45 *	0,6±0,92 #
WOMAC	1	4,04±1,70 *	1,3±0,63 #

Table. S3. **qPCR primer sequences.** Related to **STAR Methods**

	Forward	Reverse
hOPA1	GGCTCCTGACACAAAGGAAA	TCCTTCCATGAGGGTCCATT
hMFN1	ATATGGAAGACGTACGCAGAC	CCCCTGTGCTTTTTGCTTTC
hMFN2	TTGTCATCAGCTACACTGGC	AACCGGCTTTATTCCTGAGC
hDRP1	GGCGCTAATTCCTGTCATAA	CAGGCTTTCTAGCACTGAGC
hGAPDH	TGCACCACCAACTGCTTAGC	GGCATGGACTGTGGTCATGAG
mOPA1ex2-3	ATACTGGGATCTGCTGTTGG	AAGTCAGGCACAATCCACTT
mDRP1	TCAGATCGTCGTAGTGGGAA	TCTTCTGGTAAAACGTGGAC
mPGC1a	GGAATGCACCGTAAATCTGC	TTCTCAAGAGCAGCGAAAGC
mFGF21	ATGGAATGGATGAGATCTAGAGTTGG	AAGTATGTGCGAGGGCTGT
mATF4	TCCTGAACAGCGAAGTGTTG	ACCCATGAGGTTTCAAGTGC
mCHOP	GCTGGAAGCCTGGTATGAG	ATGTGCGTGTGACCTCTGTT
mGADD34	AGAGAAGACCAAGGGACGTG	CAGCAAGGAATGGACTGTG
mAtrogin-1	GCAAACACTGCCACATTCTCTC	CTTGAGGGGAAAAGTGAGACG
mBnip3	TTCCACTAGCACCTTCTGATGA	GAACACCGCATTTACAGAACAA
mCathepsinL	GTGGACTGTTCTCACGCTCAAG	TCCGTCTTCGCTTCATAGG
SMART (mFbxO21)	TCAATAACCTCAAGGCGTTC	GTTTTGCACACAAGCTCCA
mFbxO31	GTATGGCGTTTGTGAGAACC	AGCCCCAAAATGTGTCTGTA
mGabarapL	CATCGTGGAGAAGGCTCCTA	ATACAGCTGGCCCATGGTAG
mGadd34	AGAGAAGACCAAGGGACGTG	CAGCAAGGAATGGACTGTG
mGAPDH	CACCATCTTCCAGGAGCGAG	CCTTCTCCATGGTGGTGAAGAC
mltch	CCACCCACCCACGAAGACC	CTAGGGCCCGAGCCTCCAGA
mLC3b	CACTGCTCTGTCTTGTGTAGGTTG	TCGTTGTGCCTTTATTAGTGCATC
MUSA1 (mFbxO30)	TCGTGGAATGGTAATCTTGC	CCTCCCGTTTCTCTATCACG
mMuRF-1	ACCTGCTGGTGGAAAACATC	ACCTGCTGGTGGAAAACATC
mp62	CCCAGTGTCTTGGCATTCTT	AGGGAAAGCAGAGGAAGCTC
mCOXII	GCCGACTAAATCAAGCAACA	CAATGGGCATAAAGCTATGG
m18S	CATTCGAACGCTCGCCCTATCA	GGGTCGGGAGTGGGTAATTTG
mXBP1 splic	AAGAACACGCTTGGGAATGG	ACTCCCCTTGGCCTCCAC
mKlb	: ACACTGTGGGACACAACCTG	AGAGCCAACCTTCTGATGA
mFgfr1b	GAGTAAGATCGGGCCAGACA	TCACATTGAACAGGGTCAGC
mFgfr1c	GACTCTGGCCTCTACGCTTG	TCGTCGTCGTCATCATCTTC
mFgfr1	ACCAAGAAGAGCGACTTCCA	AACCAGGAGAACCCAGAGT
mFgfr4	ACTCCATCGGCCTTTCCTAC	TGTTGTCCACGTGAGGTCTT
mUCP-1	ACTGCCACACCTCCAGTCATT	CTTTGCCTCACTCAGGATTGG